



Modeling and Feedback Control for Air Flow Regulation in Deep Pits

Emmanuel Witrant, Nicolas Marchand

► To cite this version:

Emmanuel Witrant, Nicolas Marchand. Modeling and Feedback Control for Air Flow Regulation in Deep Pits. Mathematical Problems in Engineering, Aerospace and Sciences, Cambridge Scientific Publishers, 2009, 978-1-904868-70-5. hal-00982820

HAL Id: hal-00982820

<https://hal.science/hal-00982820>

Submitted on 24 Apr 2014

HAL is a multi-disciplinary open access archive for the deposit and dissemination of scientific research documents, whether they are published or not. The documents may come from teaching and research institutions in France or abroad, or from public or private research centers.

L'archive ouverte pluridisciplinaire **HAL**, est destinée au dépôt et à la diffusion de documents scientifiques de niveau recherche, publiés ou non, émanant des établissements d'enseignement et de recherche français ou étrangers, des laboratoires publics ou privés.

Modeling and Feedback Control for Air Flow Regulation in Deep Pits

Emmanuel WITRANT and Nicolas MARCHAND*

*GIPSA-lab, Control Systems Department,
Université de Grenoble, CNRS/UJF,
Grenoble, France.*

Summary. We consider the problem of regulating the air quality in underground extraction rooms for mining industry. This is a challenging control problem where the flow dynamics, the interconnections between subsystems and the time-varying topology have to be taken into account along with real-time computation constraints. Our work is focused on the deep pit part of the ventilation system, which brings fresh air at a specified pressure to the extraction levels. The flow interactions and main automation elements are first presented, with a real-time engineering model of the complete mine ventilation system. A novel control-oriented model focused on the pressure dynamics is then introduced, as a convective-resistive partial differential equation (PDE) with multiple inputs where the time-varying transport coefficients are estimated based on the distributed measurements. A fast predictive controller (FPC) is finally proposed to compensate the pressure losses due to friction and multiple flow exhausts thanks to the ventilation pit input pressure regulation. Simulation results illustrate the efficiency of the modeling and control algorithms.

1 Introduction

Mining ventilation is an interesting example of a large scale system with high environmental impact. Indeed, one of the first objectives of modern mining industry is to fulfil ecological

* E-mail: Emmanuel.Witrant, Nicolas.Marchand @gipsa-lab.grenoble-inp.fr

specifications during the ore extraction and ore crushing, by optimizing the energy consumption or the production of polluting agents. This motivates the development of new control strategies for large scale aerodynamic processes based on appropriate automation and the consideration of the global system. The approach presented in this paper is focused on the mining ventilation process, as 50 % of the energy consumed by ore extraction goes into ventilation (including heating the air). It is clear that investigating automatic control solutions and minimizing the amount of pumped air to save energy consumption (proportional to the cube of airflow quantity) is of great environmental and industrial interest.

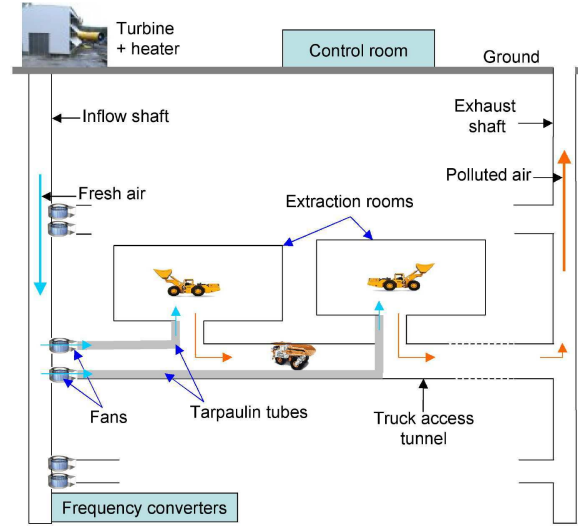


Fig. 1 Airflows in an underground mine.

The mine ventilation topology is depicted in Figure 1. It is achieved by a turbine and a heater connected on the surface to a deep pit (vertical shaft) that conducts the airflow to the extraction levels. The heater is introduced (in winter time at least) to avoid freezing in the upper part of the shaft and the air is cooled down at high depths (more than 1000 meters) because of the geothermal heating effect. From the deep pit, fans located at each extraction level pump fresh air to the extraction rooms via tarpaulin tubes. Bad quality air is naturally driven by the pressure gradient and flows from the extraction rooms back to the exhaust ventilation shaft (similar but separate from the inflow ventilation shaft).

From a control point of view, we can divide the regulation problem in two parts:

1. pressure regulation in the deep pit thanks to the ground turbine control and distributed sensors within the shaft;
2. air quality regulation in the extraction rooms thanks to the fans and chemical sensors located in the rooms.

Both problems are connected by the flow properties in the deep pit at the extraction rooms level and we consider the pressure as the interconnection variable. From a modeling point of view, the first problem typically has a clear geometry while the second one is strongly varying

in geometry (rooms are blasted every day), characteristics (tarpaulin tube length and shape) and disturbances (trucks) even within the same mine. Computational Fluid Dynamics (CFD) models, such as the one presented in [5], can then be envisioned for the deep pit while grey-box identification or global models focused on the main dynamics should be preferred for the second problem. The mine automation, communication network, historical background on real-time control and closed-loop control strategies for the second problem are detailed in [4]. The efficiency of these control strategies strongly depends on the available pressure in the vertical shaft, which is the topic of the present work. We then focus on the boundary control (turbine operation) of a deep pit flow (vertical shaft) subject to distributed losses (friction and fans exhausts).

Starting from the fundamental equation describing the flow dynamics (Navier-Stokes), we first present the simplifying hypotheses that allows the design for a real-time simulator of the complete mine aerology. This simulator is subsequently used as a reference to investigate the performance and limitations of the proposed regulation approach. Defining the pressure distribution as the regulated variable, we then propose a novel control-oriented model for large Poiseuille flows that integrates the distributed pressure measurements thanks to an online parameter identification method. The importance of a diffusive term to model the considered flow is discussed, which motivates a regulation approach focused on the convective and resistive phenomena. Based on this analysis, we finally propose a dedicated fast predictive control approach to ensure the real-time constraints and performance objectives.

This chapter is organized as follows. The physical properties and a real-time simulator of the ventilation system are presented in Section 2, along with the main physical hypotheses. A control-oriented model and an estimation method that provides for online tracking of the flow transport parameters are derived in Section 3. Section 4 is focused on a FPC feedback approach that allows for real-time pressure regulation at the bottom of the pit.

2 Ventilation in a deep pit

The aim of this section is to describe key issues that are necessary to analyse and model the airflow behavior in a deep pit. We first mention the physical principles, which provide fundamental dynamics for the mine ventilation model. This process model includes flow interactions, automation devices and can be used in real-time thanks to a 0-D modeling approach. Focusing on the pressure dynamics, we then propose a 1-D model that specifically describes the deep pit part and will be used in the next sections to set the regulation law.

2.1 Physical model

The dynamics of the flow is obtained from the conservation of mass (density ρ), momentum $\mathbf{M} = \rho\mathbf{V}$ (\mathbf{V} being the flow speed) and energy (per unit mass) E , along with the perfect gas equation of state $p = \rho RT$, where p is the pressure, R the specific gas constant and T the temperature. Choosing a *conservative* form (in the numerical sense) of Navier-Stokes equations, we have that [2]:

$$\frac{\partial}{\partial t} \begin{bmatrix} \rho \\ \rho\mathbf{V} \\ \rho E \end{bmatrix} + \nabla \cdot \begin{bmatrix} \rho\mathbf{V} \\ \rho\mathbf{V}\mathbf{V}^T \otimes \mathbf{V} + p\mathbf{I} - \varsigma \\ \rho\mathbf{V}H - \varsigma \cdot \mathbf{V} - k\nabla T \end{bmatrix} = \begin{bmatrix} 0 \\ 0 \\ \dot{q} \end{bmatrix}$$

where \otimes is the tensor product of two vectors, ς the shear stress vector, k the thermal conductivity, H the total enthalpy and $\dot{q}(x, y, t)$ the rate of heat addition (see [1] for a precise description). Neglecting the viscous effects (which is reasonable for air and the targeted simplified model), we obtain Euler equation:

$$\frac{\partial}{\partial t} \begin{bmatrix} \rho \\ \rho \mathbf{V} \\ \rho E \end{bmatrix} + \nabla \cdot \begin{bmatrix} \rho \mathbf{V}^T \otimes \mathbf{V} + p \mathbf{I} \\ \rho \mathbf{V} H \end{bmatrix} = \begin{bmatrix} 0 \\ 0 \\ \dot{q} \end{bmatrix} \quad (1)$$

A direct use of this equation to model the complete mining ventilation process involve complex CFD considerations (the airflow in the vertical shaft is mainly turbulent), typically out of reach for industrial applications and not suitable for real-time control objectives. An additional step toward model simplification and real-time computation analysis is then needed, as presented in the next subsection.

2.2 Bond graph model and real-time simulator

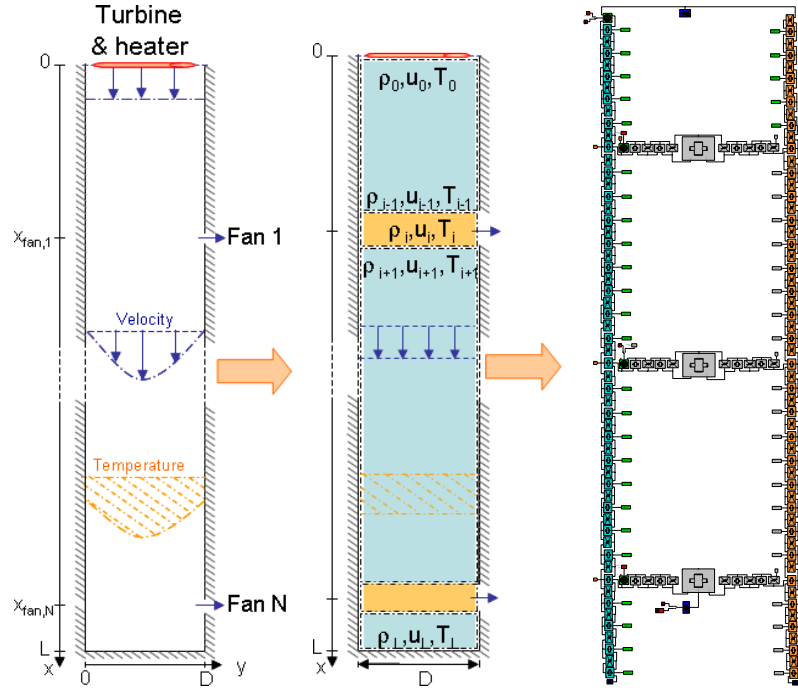


Fig. 2 2-D (left) and control-volume (middle) description of the deep pit, simulator of the complete mine aerology with three ore extraction levels (right).

This section briefly summarizes the main results presented in [5], where a non-dimensional model was proposed thanks to the bond graph approach and a real-time simulator was designed. Non-dimensional modeling has an increasing use in the design, validation and tuning

of control laws, as it allows for the integration of as much physical properties as possible (avoid data mapping) and a reduced computation time (close to real-time, approximately 10 times slower in the worst cases).

The deep pit is described by interconnected cells containing height-averaged flow values, as depicted in Figure 2. Note that this is equivalent to a control volume discretization of the flow, where a single volume is used at each height. The equivalent bond graph description is then obtained for each cell by deriving a flow/effort model from Euler equation (1) under the following hypotheses:

- H1. the impulsive term is negligible compared to the pressure: $\rho v^2 \ll p$ in the momentum equation, which is approximated with an algebraic relationship (such as Saint-Venant or Darcy-Weisbach equation) that writes as $M \approx a(M, \rho) \nabla p$, where $a(\cdot)$ is a continuously differentiable function and ∇p is the pressure gradient exerted on the control volume considered;
- H2. only the static pressure is considered, implying that the kinetic energy term in the energy conservation equation is omitted: $H = E + p/\rho$;
- H3. the gas is calorically perfect $E = c_v T$, where $c_v = R/(\gamma - 1)$ is the specific heat at constant volume and $\gamma = 1.4$.

The mine ventilation simulator is constructed based on this flow description and the fans models proposed in [3]. The deep pits (inflow and exhaust) are both discretized with 28 control volumes and we consider three extraction levels. The turbine and fans regulation is done by setting their rotational speed, and flow speed, pressure and temperature can be measured in each control volume. The resulting computation time is 34 times faster than real-time in an *Intel Centrino® 1.83 GHz PC*. This simulator is used in the next sections to illustrate the estimation and control strategies. It may also be considered in the futur to develop virtual sensing capabilities in real-time operation schemes.

2.3 Distributed pressure dynamics

For real-time control purposes, we are specifically interested in the pressure dynamics, which provides for the regulated variable. In order to achieve model-based feedback control, the distributed measurements can be used to reduce the model complexity thanks to on-line parameter estimation, as described in the next section. The appropriate simplified model is obtained from H1-H3 by expressing the energy equation in terms of pressure (perfect gas equation) as:

$$\begin{aligned} \frac{\partial \rho E}{\partial t} &= -\frac{\partial}{\partial x} \left[M \cdot \left(E + \frac{p}{\rho} \right) \right] + \dot{q} \\ \Leftrightarrow \frac{\partial p}{\partial t} &= -\frac{\partial}{\partial x} \left[\frac{M}{\rho} \cdot \left(1 + \frac{R}{c_v} \right) p \right] + \frac{R}{c_v} \dot{q} \end{aligned} \quad (2)$$

Note that the momentum can be obtained by implicit resolution of the Darcy-Weisbach equation, which then provides the dynamics for the density evolution.

3 Distributed measurements and online parameters estimation

As mentioned previously, we suppose that distributed measurements (i.e. obtained thanks to a wireless sensor network) are available to set the control law. One of the main advantages is the

possibility to constrain the pressure model according to the measured behavior of the flow. In this section, we derive a generic model architecture from (2) that depicts convective-resistive dynamics. An online parameter estimation method is then introduced to set the transport coefficients according to distributed measurements.

3.1 Control oriented model

To propose an efficient model-based control of the flow dynamics, we need to capture the main tendencies of the pressure evolution. The momentum and density impact on the pressure dynamics are considered with their volume-averaged values:

$$\bar{M}(t) = \frac{1}{\mathcal{V}} \oint_{\mathcal{V}} M(v, t) dv, \quad \bar{\rho}(t) = \frac{1}{\mathcal{V}} \oint_{\mathcal{V}} \rho(v, t) dv$$

where \mathcal{V} corresponds to the volume of the pit. The energy losses are generated by pressure losses at the exhausts locations and friction on the walls, which implies that:

$$\frac{R}{c_v} \dot{q}(x, t) = s(t) \varrho_x(x) f_{fan}(\Delta p_{fan}(t), \eta(t)) + r(t) p(x, t)$$

where s quantifies the impact of the exhausts on the main flow, ϱ_x is set by the mine topology (i.e. $\varrho_x = 1$ at the exhausts location and 0 otherwise), f_{fan} depends on the fan model, the vector Δp_{fan} contains the pressure gradients across each fan, η is the blades rotational speed and r denotes the resistance on the pit sides. ϱ_x , Δp_{fan} and η are considered as known engineering parameters. The physical model (2) is then approximated with the averaged control-oriented model:

$$\bar{p}_t = c(t) \bar{p}_x + r(t) \bar{p} + s(t) p_{ext}(x, t) \quad (3)$$

where $c(t) \doteq -\bar{M}(t)/\bar{\rho}(t) \cdot (1 + R/c_v)$, $p_{ext}(x, t) \doteq \varrho_x(x) f_{fan}(\Delta p_{fan}(t), \eta(t))$ and $p_y \doteq \partial p / \partial y$. The boundary conditions are set by the inflow pressure $\bar{p}(0, t) = p_{in}(t)$ (regulated thanks to a local PID feedback on the turbine rotation speed) and the dead end at the bottom of the shaft $\bar{p}_x(L, t) = 0$, L being the shaft length.

3.2 Online parameter estimation

A classical estimation problem is to find the set of parameters ϑ that minimizes the difference between the measured and estimated data, given a specific model architecture. This is done in this section by deriving a variation law for ϑ such that the estimation error is exponentially decreasing. We consider the general class of systems that involve transport phenomena described as:

$$p_t = d(t) p_{xx} + c(t) p_x + r(t) p + s(t) p_{ext}(x, t) \quad (4)$$

where $\vartheta(t) = \{d(t), c(t), r(t), s(t)\}$ denote the diffusive, convective, resistive and source coefficients, respectively, and $p_{ext}(x, t)$ is a distributed source term. The boundary conditions are given by $p(0, t) = p_0(t)$ and $p_x(L, t) = 0$, for $x \in [0, L]$. The variation of ϑ is provided by the following theorem.

Theorem 1. Consider the general class of systems described by:

$$\begin{cases} p_t = \mathcal{A}(p, p_x, p_{xx}, u, \vartheta)\vartheta \\ a_1 p_x(0, t) + a_2 p(0, t) = a_3 \\ a_4 p_x(L, t) + a_5 p(L, t) = a_6 \end{cases} \quad (5)$$

where p is the state, u a known exogenous input, $\vartheta \in \mathbb{R}^M$ denotes a set of time-varying parameters, $\mathcal{A}(p, p_x, p_{xx}, u, \vartheta) \in \mathbb{R}^{1 \times M}$ sets the input-to-state relationship and a_i are scalar real coefficients. The estimated state $\hat{p}(x, t)$ converges exponentially to $p(x, t)$ in the \mathcal{L}_2 sense and:

$$\|p(x, t) - \hat{p}(x, t)\|_2^2 = e^{-2(\gamma+\lambda)t} \|p(x, 0) - \hat{p}(x, 0)\|_2^2$$

where $\|\cdot\|_2$ denotes the \mathcal{L}_2 norm and γ, λ are positive scalar parameters, if:

$$\begin{cases} \hat{p}_t = \mathcal{A}(\hat{p}, \hat{p}_x, \hat{p}_{xx}, u, \hat{\vartheta})\hat{\vartheta} + \gamma(p - \hat{p}) \\ a_1 \hat{p}_x(0, t) + a_2 \hat{p}(0, t) = a_3 \\ a_4 \hat{p}_x(L, t) + a_5 \hat{p}(L, t) = a_6 \\ \hat{\vartheta} = \mathcal{A}(\hat{p}, \hat{p}_x, \hat{p}_{xx}, u, \hat{\vartheta})^\dagger [p_t + \lambda(p - \hat{p})] \end{cases} \quad (6)$$

where A^\dagger is the Moore-Penrose inverse of A .

Proof. Considering the estimation error $\epsilon(x, t) \doteq p(x, t) - \hat{p}(x, t)$, we have from (6) that:

$$\epsilon_t = p_t - [p_t + \lambda(p - \hat{p}) + \gamma(p - \hat{p})] = -(\gamma + \lambda)\epsilon$$

with the boundary conditions $\epsilon(0, t) = 0$ and $\epsilon_x(L, t) = 0$. Then, to investigate the stability in the \mathcal{L}_2 sense, we introduce the *Lyapunov* function:

$$\mathcal{L}(t) \doteq \frac{1}{2} \int_0^L \epsilon^2 dx$$

It follows that:

$$\frac{d\mathcal{L}}{dt} = -(\gamma + \lambda) \int_0^L \epsilon^2 dx = -2(\gamma + \lambda)\mathcal{L}$$

which directly implies that $\|\epsilon(x, t)\|_2^2 = e^{-2(\gamma+\lambda)t} \|\epsilon(x, 0)\|_2^2$ and concludes the proof.

Remark 1. The parameter λ is introduced to moderate the variations of $\hat{\vartheta}$ and γ ensures the convergence of the estimated dynamics. The use of two parameters instead of one, which would be sufficient from a stability point of view, is motivated by the need to adjust the estimator performances according to robustness constraints and non-smooth signal variations.

Example 1. Consider the model (4) with the inputs depicted in Figure 3, a Dirichlet boundary condition at the surface and a Neumann one at $x = L$. Such a model writes as (5) with:

$$\begin{cases} \mathcal{A}(p, p_x, p_{xx}, u, \vartheta) = [p_{xx} \ p_x \ p \ p_{ext}] \\ \vartheta = [d \ c \ r \ s]^T \\ a_1 = 0, \ a_2 = 1, \ a_3 = p_{in} \\ a_4 = 1, \ a_5 = a_6 = 0 \end{cases}$$

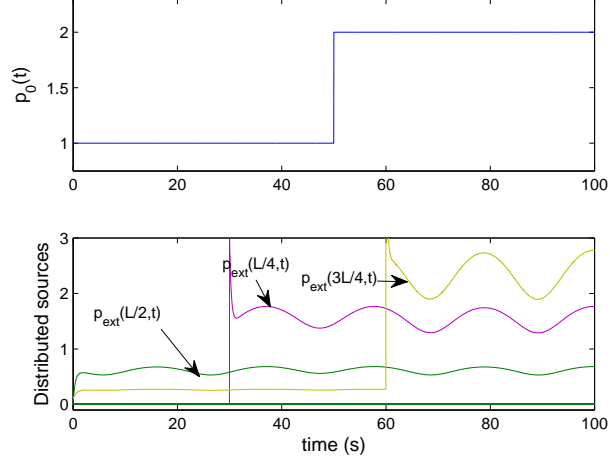


Fig. 3 Boundary condition and distributed outputs.

and the estimated values of the transport coefficients $\hat{\vartheta}$ are directly obtained according to (6). The corresponding algorithm is designed by discretizing the diffusivity using central difference and the conductivity thanks to a Lax-Wendroff scheme (the model thus remains stable for $d(t) = 0$, provided that the conditions on the associated Courant number are satisfied). The reference model algorithm is set by introducing $P \in \mathbb{R}^N$ as the vector of discretized pressures and with the variation law:

$$\begin{aligned}
 P_1^{k+1} &= P_1^k + t_s \left[\frac{d}{\Delta x^2} \mathcal{D}(p_0, P_1, P_2) + \frac{c}{\Delta x} \mathcal{C}(p_0, P_1, P_2, \alpha) + rP_1 + sP_{ext,1} \right] \\
 &\vdots \\
 P_i^{k+1} &= P_i^k + t_s \left[\frac{d}{\Delta x^2} \mathcal{D}(P_{i-1}, P_i, P_{i+1}) + \frac{c}{\Delta x} \mathcal{C}(P_{i-1}, P_i, P_{i+1}, \alpha) + rP_i + sP_{ext,i} \right] \\
 &\vdots \\
 P_N^{k+1} &= P_N^k + t_s \left[\frac{d}{\Delta x^2} \mathcal{D}(P_{N-1}, P_N, P_N) + \frac{c}{\Delta x} \mathcal{C}(P_{N-1}, P_N, P_N, \alpha) + rP_N + sP_{ext,N} \right]
 \end{aligned}$$

with:

$$\begin{aligned}
 \mathcal{D}(P_{i-1}, P_i, P_{i+1}) &\doteq P_{i-1} - 2P_i + P_{i+1} \\
 \mathcal{C}(P_{i-1}, P_i, P_{i+1}, \alpha) &\doteq \frac{\alpha - 1}{2} P_{i-1} - \alpha P_i + \frac{\alpha + 1}{2} P_{i+1}
 \end{aligned}$$

where P_i , $i = 2 \dots N - 1$ denotes the i^{th} component of P , k the time index, t_s the sampling time, $-\alpha = -ct_s/\Delta x$ the CFL number and Δx the spatial step. The estimated pressure vector \hat{P} is computed using a similar algorithm and the parameter estimation is achieved with:

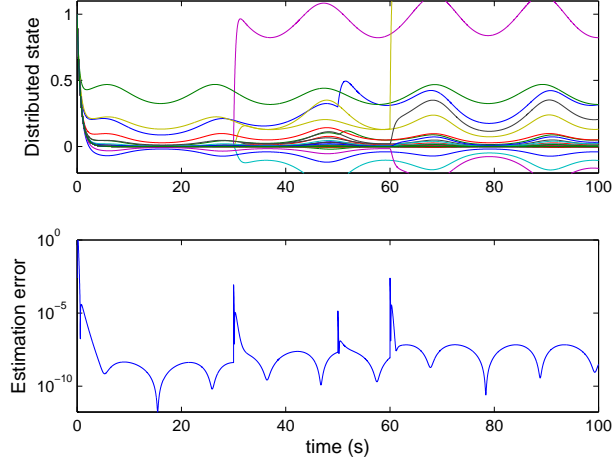


Fig. 4 Model pressure $P(t)$ and squared estimation error $\|\epsilon(x, t)\|_2^2$.

$$\mathcal{A} = \begin{bmatrix} \frac{1}{\Delta x^2} \mathcal{D}(p_0, \hat{P}_1, \hat{P}_2) & \frac{1}{\Delta x} \mathcal{C}(p_0, \hat{P}_1, \hat{P}_2, \hat{\alpha}) & \hat{P}_1 & P_{ext,1} \\ \vdots & \vdots & \vdots & \vdots \\ \frac{1}{\Delta x^2} \mathcal{D}(\hat{P}_{i-1}, \hat{P}_i, \hat{P}_{i+1}) & \frac{1}{\Delta x} \mathcal{C}(\hat{P}_{i-1}, \hat{P}_i, \hat{P}_{i+1}, \hat{\alpha}) & \hat{P}_i & P_{ext,i} \\ \vdots & \vdots & \vdots & \vdots \\ \frac{1}{\Delta x^2} \mathcal{D}(\hat{P}_{N-1}, \hat{P}_N, \hat{P}_N) & \frac{1}{\Delta x} \mathcal{C}(\hat{P}_{N-1}, \hat{P}_N, \hat{P}_N, \hat{\alpha}) & \hat{P}_N & P_{ext,N} \end{bmatrix}$$

The resulting model pressure and estimation error are depicted in Figure 4 while the exact and estimated values of the transport coefficients are presented in Figure 5. We can see that the proposed estimator achieves a very precise tracking of the transport parameters and quickly converges to the exact values. The large perturbations induced by the steps in the boundary and distributed input signals are reflected as peaks in the estimated parameters (at 30, 50 and 60 s) but are quickly damped.

3.3 Application to the mining ventilation case

The test case is defined as follows, for three extraction levels in a $L = 1100$ m deep mine. The 1st level fan (at $L/4$) is not operated (a small flow is naturally driven by the pressure gradient), the 2nd level fan (at $L/2$) goes from 0 to 150 rpm at $t = 2000$ s and the 3rd level fan (at $3L/4$) is operated at 200 rpm. A step is set on the turbine rotation speed at $t = 1000$ s. Pressure measurements at the turbine output and at the bottom of the pit are available for feedback control and presented in Figure 7 (top). We consider two different estimated models, with:

1. four transport parameters: diffusion, convection, resistance and source;
2. three parameters, excluding the diffusion according to (3).

The resulting estimation error and parameters values can be compared in Figures 6 and 7, respectively. We can see that the estimation error quickly decreases to a negligible value in

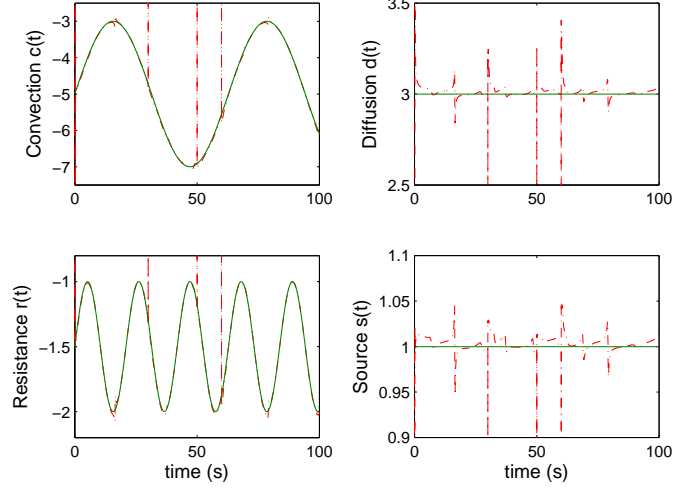


Fig. 5 Exact (‘—’) and estimated (‘- -’) transport coefficients values.

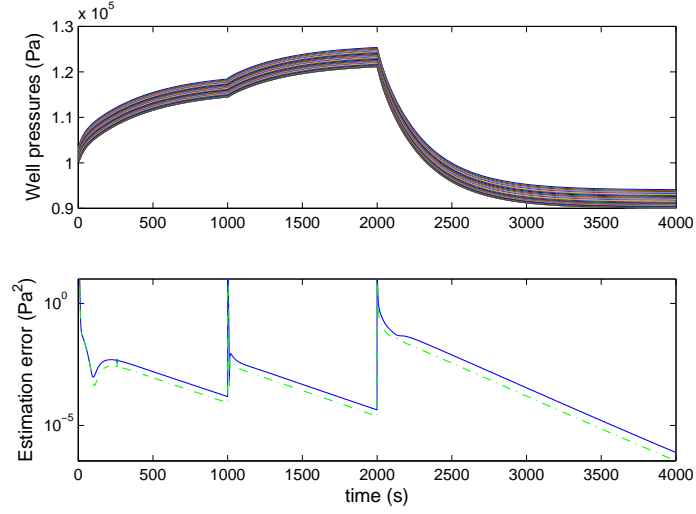


Fig. 6 Pressure profiles and squared estimation error (three ‘—’ and four ‘- -’ parameters).

both cases, which validates the proposed estimation strategy. Furthermore, the slight estimation improvement obtained thanks to the additional diffusive term, noticeable but not crucial, validates the volume-averaging of the momentum and density as a possible model simplification for feedback control.

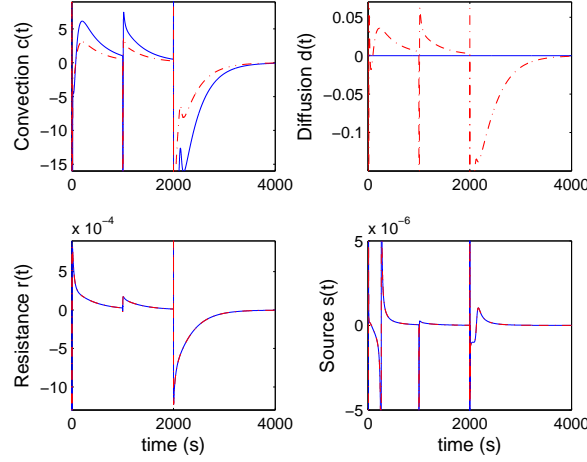


Fig. 7 Parameter estimation for the mine ventilation shaft (three ‘—’ and four ‘- - -’ parameters).

4 Fast model predictive control

We consider that the heater is operated based on the atmospheric conditions (i.e. it acts as an external input) and that the regulated input is the turbine downflow pressure (a local control loop is set on the turbine to adjust its rotational speed according to a desired pressure). The control problem is then to ensure a minimum pressure within the shaft (at each extraction level) based on the turbine actuation. As the pressure can only decrease as we go deeper, the control objective can be reduced to ensuring a minimum pressure at the bottom of the pit. We consider that distributed pressure measurements are available to set the state feedback control law.

The aim of this section is to propose a predictive control of the mine process. Predictive control is widely used in process industry because of the usual robustness of the method and of the slow dynamics of the processes. Classical predictive control requires the optimization of a criterium whose optimum gives the control to apply over the next time instant. Unfortunately, predictive control relies on finding the extremum of an optimization problem that can hardly be guaranteed, especially for systems described by PDE like the present system. Recently, fast predictive control approaches were developed that enable to have an analytical solution to the predictive control problem without any optimization by using the structure of the system. This is what we propose to apply here.

We start from the control oriented model and assume that the time varying parameters $c(t)$, $r(t)$ and $d(t)$ and external disturbance $s(t)p_{ext}(x, t)$ are slowly varying parameters and can therefore be considered as constants: $c(t) = c$, $r(t) = r$, $d(t) = d$ and $s(t)p_{ext}(x, t) = sp_{ext}(x)$. By slowly varying, it is only necessary to assume that the perturbation related to the opening and closing of the extraction rooms levels $p_{ext}(x)$ is piecewise constant. The diffusive term d is assumed to be small and is neglected: $d \approx 0$. Note that these assumptions are only made to design the control law that is tested and applied to the global system without any simplifications. Therefore, we focus on the following equation:

$$p_t = cp_x + rp + sp_{ext}(x) \quad (7)$$

Predictive control consists in finding an open-loop control profile $\tau \rightarrow p(0, \tau)$ at each instant t such that the solution of the dynamical system (here the solution of (7)) has “some” properties on a time horizon $[t, t + w]$ where w is the prediction horizon (may be infinite). These properties can be very various and have to ensure the stability of the closed loop scheme. The most classical property is optimality in optimal predictive control. This open-loop control profile is applied at its first instant $p(0, 0)$ and the scheme is repeated at the next time instant $t + dt$.

The aim of the control law is to give the inflow pressure control profile $p(0, \tau)$ in order to ensure a given down pressure $p(L, \infty)$ in closed loop. Once the steady state has been achieved, a corresponding constant inflow pressure $p(0, \infty)$ will ensure the desired down pressure $p(L, \infty)$. At time t , we assume that the system starts with some constant initial inflow $p(0, t)$, an established pressure profile in the ventilation pit and $p(L, t)$ at the bottom. This established steady state field of pressure $p_{st}(x, p_0)$ results from the application of the constant inflow pressure p_0 and is simply given by (7) assuming no time derivatives, that is:

$$p_{st}(x, p_0) = p_0 e^{-\frac{r}{c}x} - \frac{s}{c} \int_0^x e^{-\frac{r}{c}(x-z)} p_{ext}(z) dz$$

Note that according to this notation, one has $p(L, \infty) = p_{st}(L, p(0, \infty))$ and, as soon as the system is in a steady state regime at time t , $p(L, t) = p_{st}(L, p(0, t))$.

We propose to approximate the pressure open-loop profile $p(x, t + \tau)$, $\tau \in [0, +\infty]$, by:

$$\tilde{p}(x, t + \tau) = p e^{-\alpha x} e^{-\beta \tau} + p_{st}(x, p(0, \infty))$$

When τ increases, $\tilde{p}(x, t + \tau)$ then converges to the steady state solution that ensures the desired down pressure $p(L, \infty)$. At time t ($\tau = 0$), it is natural to take:

$$p = e^{\alpha L} [p(L, t) - p_{st}(L, p(0, \infty))]$$

in order to ensure the initial condition at least at $x = L$. Finally, to ensure that \tilde{p} is a solution of (7), we impose that $\beta = \alpha c - r$.

In this scheme, α is a free parameter. However:

- $\alpha > r/c$ is necessary to ensure the convergence of the open-loop trajectory to $p(L, \infty)$;
- the convergence speed is inversely proportional to the difference between α and r/c ;
- the closer α is to r/c , the closer $\tilde{p}(x, t)$ is to $p(x, t)$, that is to the exact solution of (7).

The open-loop control law profile, defined at time t for any $\tau > 0$, is therefore given by:

$$\tilde{p}(0, t + \tau) = (p(L, t) - p(L, \infty)) e^{-\alpha(x-L)} e^{-\beta \tau} + p(0, \infty)$$

where $p(L, t)$ is the current down pressure, $p(L, \infty)$ is the desired down pressure and:

$$p(0, \infty) = e^{\frac{r}{c}L} \left[p(L, \infty) + \frac{s}{c} \int_0^L e^{-\frac{r}{c}(L-z)} p_{ext}(z) dz \right]$$

To prove the efficiency of the proposed approach, two scenarii are compared:

1. the inflow pressure is set at some value that ensures a down pressure of 1 hPa for the initial ventilation topology;
2. the inflow pressure is automatically computed and adapted online according to the above control law using the down pressure measurement.

In both cases, we consider the test case described in Subsection 3.3 with the 2nd level fan operated at $t = 1000$ s instead of $t = 2000$ s. The obtained control is actually not directly set on the system but acts as a reference to the turbine outflow pressure. Indeed, the shaft inflow pressure is set using the corresponding turbine speed by means of a local control law (proportional-integral control) on the turbine.

On Figure 8, one can see the desired and real inflow pressure as well as its corresponding down pressure. The control law clearly enables 1) a fastest convergence to the desired down pressure and 2) to maintain the down pressure even in case of fan operation at different extraction levels.

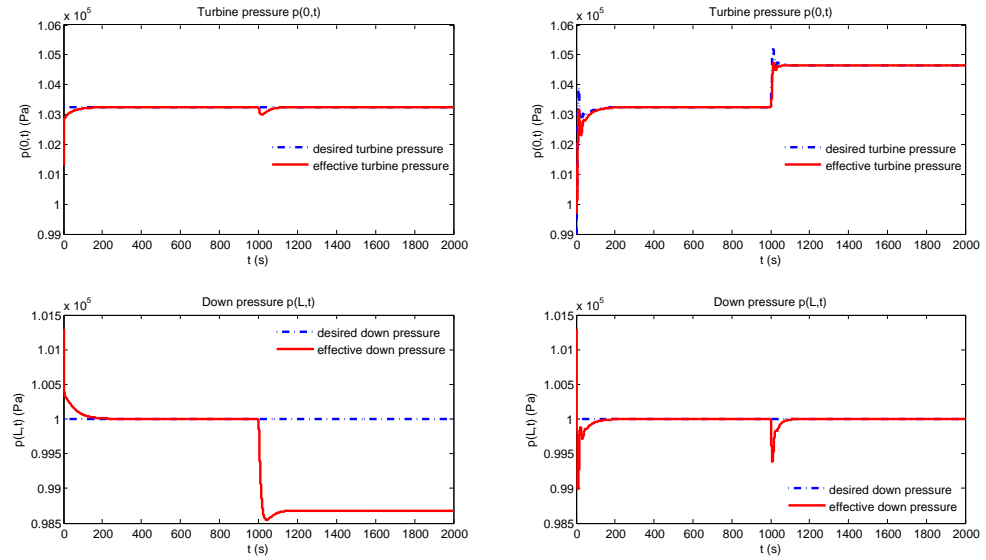


Fig. 8 Down pressure regulation in a mine with (right) and without (left) fast predictive control

Conclusions

In this work, we considered the problem of airflow modeling and control in deep pits, such as the ones encountered in mines. Starting from the fundamental physical equations of the flow and engineering models of the automation components, we first proposed a real-time model of the complete mine aerology based on a bond graph approach. Specific hypotheses related to the flow properties were then expressed to obtain a 1-D model of the pressure dynamics.

It was then shown that, considering the averaged impact of the momentum and density, the pressure dynamics could be reduced to a transport equation with time-varying coefficients. A

specific estimation method was derived to infer these coefficients from the distributed pressure measurements and the interest for a diffusive term in the flow model was discussed. A model-based feedback control approach based on fast predictive control was proposed. Thanks to this approach, a reference down pressure can be ensured even in case of pressure perturbation due to air usage for underground extraction rooms.

The overall results illustrate the validity of simplified models and the interest for dedicated model-based control methodologies to regulate large airflows, thus allowing for an increased security and a reduced energy consumption. The proposed theoretical results on flow model simplification, transport parameters estimation and FPC for boundary regulation can be applied more widely on large Poiseuille flows with distributed outputs.

References

1. J.M.B. Brown, A.E. Vardy, and A.S. Tijsseling. Response of wall heat transfer to flows along a cylindrical cavity and to seepage flows in the surrounding medium. Technical report, Eindhoven: Technische Universiteit Eindhoven, 2005.
2. C. Hirsch. *Numerical Computation of Internal & External Flows: the Fundamentals of Computational Fluid Dynamics*. Butterworth-Heinemann (Elsevier), 2nd edition, 2007.
3. V. Talon and S. Cstric. Engine control model based design with achille library. *E-COM: Rencontres scientifiques de l'IFP*, pages 33–51, October 2006.
4. E. Witrant, A. D'Innocenzo, G. Sandou, F. Santucci, M.D. Di Benedetto, A.J. Isaksson, K.H. Johansson, S.I. Niculescu, S. Olaru, E. Serra, S. Tennina, and U. Tiberi. Wireless ventilation control for large-scale systems: the mining industrial case. *International Journal of Robust and Nonlinear Control*, 2009.
5. E. Witrant, K.H. Johansson, and the HynX team. Air flow modelling in deep wells: application to mining ventilation. In *Proc. of the IEEE Conference on Automation Science and Engineering (CASE 2008)*, Washington DC, USA, August 2008.